Environmental Research Letters



OPEN ACCESS

RECEIVED

31 July 2018

REVISED

14 November 2018

ACCEPTED FOR PUBLICATION 20 November 2018

PUBLISHED

21 January 2019

Original content from this work may be used under the terms of the Creative Commons Attribution 3.0 licence.

Any further distribution of this work must maintain attribution to the author(s) and the title of the work, journal citation and DOI.



LETTER

The impact of aerosol–radiation interactions on the effectiveness of emission control measures

Mi Zhou¹, Lin Zhang^{1,6}, Dan Chen^{2,6}, Yu Gu^{3,4}, Tzung-May Fu¹, Meng Gao⁵, Yuanhong Zhao¹, Xiao Lu¹, and Bin Zhao³

- ¹ Laboratory for Climate and Ocean-Atmosphere Studies, Department of Atmospheric and Oceanic Sciences, School of Physics, Peking University, Beijing 100871, People's Republic of China
- ² Institute of Urban Meteorology, Beijing 100089, People's Republic of China
- Joint Institute for Regional Earth System Science and Engineering and Department of Atmospheric and Oceanic Sciences, University of California, Los Angeles, CA 90095, United States of America
- ⁴ University of California, Los Angeles Institute for Technology Advancement, Suzhou Industrial Park (UCLA ITA SIP), Suzhou, People's Republic of China
- School of Engineering and Applied Sciences, Harvard University, Cambridge, MA 02138, United States of America
- ⁶ Authors to whom any correspondence should be addressed.

E-mail: zhanglg@pku.edu.cn and dchen@ium.cn

Keywords: particulate matter, $PM_{2.5}$, aerosol–radiation interaction, aerosol effect, emission control, air pollution Supplementary material for this article is available online

Abstract

Temporary emission control measures in Beijing and surrounding regions have become a prevailing practice to ensure good air quality for major events (e.g. the Asia-Pacific Economic Cooperation (APEC) Summit on 5–11 November 2014) and to mitigate the severity of coming pollution episodes. Since $PM_{2.5}$ affects meteorology via aerosol–meteorology interactions, a question arises how these interactions may impact the response of $PM_{2.5}$ to emission reductions and thus the effectiveness of emission control measures. Here we use the coupled meteorology-chemistry model WRF-Chem to investigate this issue with focus on aerosol–radiation interactions (ARI) for the APEC week and three more polluted episodes over North China. We find a quadratic relationship between $PM_{2.5}$ concentration changes due to emission reductions and $PM_{2.5}$ levels, instead of an approximately linear response in the absence of ARI. The ARI effects could only change the effectiveness of emission control by 6.7% during APEC in Beijing, but reach 21.9% under more polluted conditions. Our results reveal that ARI can strongly affect the attribution of $PM_{2.5}$ variability to emission changes and meteorology, and is thus important for assessing the effectiveness of emission control measures.

1. Introduction

The North China Plain, particularly the Beijing—Tianjin—Hebei (BTH) region, has been experiencing heavy PM_{2.5} air pollution in recent years, causing public concerns on human health (Lelieveld *et al* 2015, Zhang *et al* 2015a, Zhong *et al* 2018). In order to ensure good air quality for major events such as the Asia-Pacific Economic Cooperation (APEC) Summit on 5–12 November 2014, the Chinese government has enforced temporary emission control measures in Beijing and surrounding regions. More recently, such practices have been further adopted to inhibit the formation of regional haze in Beijing and to reduce its potential damage to the society. Previous analyses of these temporary practices have shown that meteorological conditions are important for determining PM_{2.5} concentration reductions and thus the effectiveness of emission control measurements (Guo *et al* 2016, Zhang *et al* 2016, Sun *et al* 2016, Liang *et al* 2017).

PM_{2.5} in turn affects local meteorology via aero-sol-meteorology interaction at short time scales (Wang *et al* 2014). Aerosols can directly scatter or absorb solar radiation (Hansen *et al* 1997), leading to perturbations in the energy budget (Ramanathan *et al* 2001), which is defined as aerosol-radiation interactions (ARI hereafter). Both scattering and absorbing aerosols can increase atmospheric stability (Qiu *et al* 2017). In addition, aerosols can serve as sources of cloud condensation nucleus, altering cloud lifetime

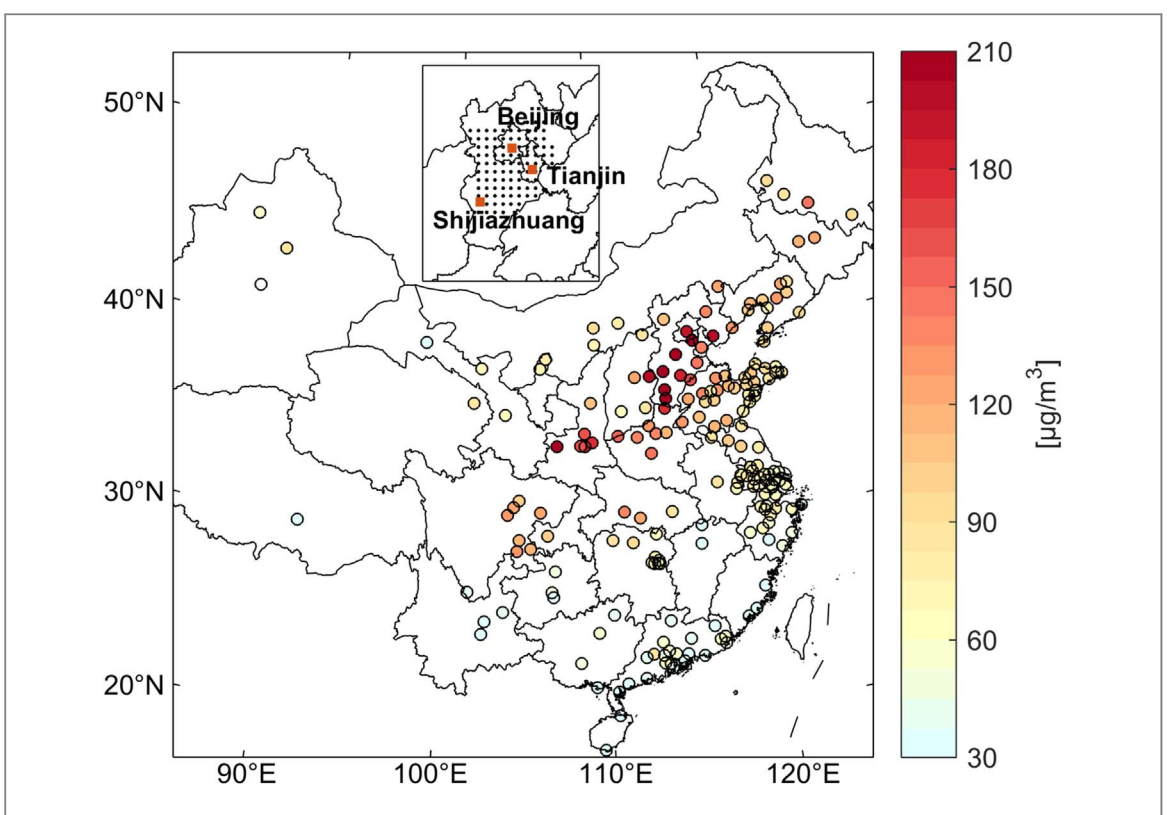


Figure 1. Modeling domain with a horizontal grid resolution of 36 km over China. Also shown are observed mean surface $PM_{2.5}$ concentrations during 17–26 February 2014 (Ep1 in table 2). The small panel on the top shows the locations of Beijing, Tianjin, and Shijiazhuang city centers (red squares), the model grids (black dots, 36 km resolution) representing the BTH region in this study, and the nested domain in additional sensitivity experiments.

and albedo, as well as precipitation (Andreae *et al* 2008). This is known as aerosol–cloud interactions (ACI hereafter). Both ARI and ACI can alter the lapse rate and vertical mixing of mass and momentum in the planetary boundary layer (PBL) (Yang *et al* 2016), and perturb meteorological variables such as surface temperature, relative humidity (RH), wind, and PBL height (PBLH) (Gao *et al* 2015). Consequently, these perturbations affect PM_{2.5} concentrations via changes in transport and chemical formation (Yang *et al* 2015, Zhang *et al* 2015b, Chen *et al* 2016, Qiu *et al* 2017, Li *et al* 2017a).

Previous studies have shown that aerosolmeteorology interactions can strongly impact PM_{2.5} concentrations during pollution episodes (Wang et al 2014) as well as for monthly averages (Zhao et al 2017, Zhang et al 2018). One question remaining largely unexplored is that how these interactions would respond to temporary emission control measures. This is of great importance to assess the effectiveness of emission control measures on reducing PM_{2.5}. Here we use the coupled meteorology-chemistry model WRF-Chem to address this issue. A recent WRF-Chem modeling study has found that the ACI effects are much smaller than ARI over the BTH region in fall and winter (Zhang et al 2018), when severe haze episodes occur frequently. Besides, ACI effects are highly uncertain in current models (Boucher et al 2013). Thus, we will focus on ARI effects and analyze the APEC time period

as well as three other PM_{2.5} pollution episodes when emission control policy might be an urgent need.

2. Methodology

2.1. The WRF-Chem model

WRF-Chem is an online-coupled meteorology-chemistry model that simulates transformation of chemical species (both trace gases and aerosols), along with meteorological fields and their interactions (Grell et al 2005, Fast et al 2006, Gustafson et al 2007, Chapman et al 2009). We use WRF-Chem version 3.6.1 in this study. Figure 1 shows the modeling domain of this study covering most of China with a horizontal resolution of 36 km and 37 vertical levels extending from the surface to 50 hPa. Meteorological initial and lateral boundary conditions are provided by the National Centers for Environmental Prediction (NCEP) FNL (Final) Operational Global Analysis data at $1^{\circ} \times 1^{\circ}$ resolution. The initial and boundary chemical conditions are archived from the global MOZART (Model for OZone And Related chemical Tracers) model.

The following physical and chemical schemes are used in WRF-Chem: the RRTMG scheme for shortwave and longwave radiation, the Morrison aerosol microphysics scheme (Morrison *et al* 2005), the Noah land surface scheme (Chen *et al* 2001), the Yonsei University PBL scheme (Hong *et al* 2006), the 4-bin



version of model for simulating aerosol interactions and chemistry (MOSAIC) for aerosol (Zaveri *et al* 2008) and CBMZ (Zaveri *et al* 1999) for gas-phase chemistry. MOSAIC employs the size bin treatment (0.039–0.156, 0.156–0.625, 0.625–2.5, and 2.5–10.0 μ m for dry diameter) for aerosol species including sulfate (SO₄ ²–), nitrate (NO₃–), ammonium (NH₄+), black carbon (BC), organic carbon (OC), and other inorganic mass (OIN). Aerosols are assumed to be internally mixed inside each bin. Secondary organic aerosols are not included in this study.

ARI effects are simulated using parameters such as aerosol optical depth, single scattering albedo, and asymmetry factor in the model calculation of radiation transfer (Chapman et al 2009). Aerosol optical properties are calculated based on the chemical composition, size distribution, mass concentration, and mixing rule (Fast et al 2006). The Morrison microphysics scheme simulates ACI via linking prognostic aerosols to cloud condensation nuclei. We use a prescribed cloud droplet number concentration (CDNC) of 10 cm⁻³ in the Morrison microphysics scheme to exclude ACI as well as anthropogenic impacts on clouds (Zhao et al 2017, Zhang et al 2018). Although the CDNC value of 10 cm⁻³ does not represent the BTH condition, sensitivity simulations with CDNC of 200 cm⁻³ as will be discussed below show minor changes on our results.

For the anthropogenic emissions, we use the multi-resolution emission inventory of China for the year 2012 and the 2010 MIX Asian Emission Inventory (Li et al 2017b) for the rest of the Asian domain. These inventories provide monthly anthropogenic emissions of primary PM_{2.5} and its precursors from power plant, industry, residential, transportation, and agriculture sectors. Natural dust emissions follow the GOCART scheme with Air Force Weather Agency (AFWA) modifications (Jones et al 2012). Biogenic nonmethane VOC emissions are calculated in the model using the Model of Emissions of Gases and Aerosols from Nature (MEGAN) algorithm (Guenther et al 2006).

2.2. Model sensitivity simulations

We analyze four pollution episodes occurred over BTH (Ep1: 17–26 February 2014, Ep2: 21–25 October 2014, Ep3: 05–11 November 2014, and Ep4: 18–24 December 2015). We use hourly PM_{2.5} mass concentration measurements from the China National Environmental Monitoring Center network (http://106.37. 208.233:20035/). The four episodes are at different pollution levels and cover a wide range of PM_{2.5} concentrations in Beijing (observed episodic means of 49–188 μ g m⁻³). Figure 1 also shows observed mean surface PM_{2.5} concentrations during 17–26 February 2014 (Ep1). A heavy haze occurred over BTH with a regional mean PM_{2.5} concentration of 199 μ g m⁻³. To evaluate the model simulated PM_{2.5} concentrations, we conduct a base simulation for 2–27 February 2014,

Table 1. Configurations for model sensitivity simulations.

Run	Emission reduction	ARI	ACI
A	off	On	Off
В	on	On	Off
С	off	Off	Off
D	on	Off	Off

13 October–12 November 2014, and 9–24 December 2015 covering the four episodes. The first two days for each period are used for spin-up and are not analyzed. Both ARI and ACI are turned on in the base simulation. Anthropogenic emissions are unchanged except for the APEC period when emission control measures were applied over 2–12 November 2014. Table S1, available online at stacks.iop.org/ERL/14/024002/mmedia, lists the percentages of emission reduction due to the control measures. Emission reductions are estimated by the Beijing Municipal Environmental Protection Bureau (BMEPB) (BMEPB 2014) for Beijing, and by Guo *et al* (2016) for nearby regions (Tianjin, Inner Mongolia, Hebei, Shanxi, and Shandong).

We conduct four sensitivity simulations for each episode by turning on/off ARI and with/without emission reduction to investigate the impact of ARI on the effectiveness of emission control measures, while ACI are turned off in all sensitivity simulations. We assume that the same control measures and associated emission reductions in APEC (table S1) could applied to other episodes. Table 1 summarizes the model settings for the sensitivity simulations. We can thus attribute for each episode the difference between Run C and Run A to the effects of ARI without emission controls, and the difference between Run D and Run B to the ARI effects with reduced anthropogenic emissions. Here we define the weakened ARI effects due to reduced emission as Δ ARI $_V$:

$$\Delta ARI_V = (V_B - V_D) - (V_A - V_C),$$
 (1)

where V represents $PM_{2.5}$ concentration or meteorological variables such as PBLH, surface wind speed (WS), surface wind direction (WD), and RH. For $PM_{2.5}$, we can also estimate the impact of emission control measures with ARI considered ($\Delta PM_{2.5}$) as the difference between Run A and Run B, and the impact if there were no ARI ($\Delta PM_{2.5}^*$) as the difference between Run C and Run D. We then define the ratio of $\Delta ARI_{PM2.5}/\Delta PM_{2.5}$ as a metric to quantify the impact of ARI on the effectiveness of emission control measures.

3. Results and discussion

3.1. Measured and model simulated PM_{2.5} concentrations

Figure 2 compares the measured and model simulated hourly PM_{2.5} concentrations at three megacities (Beijing, Tianjin, and Shijiazhuang; figure 1) in BTH during



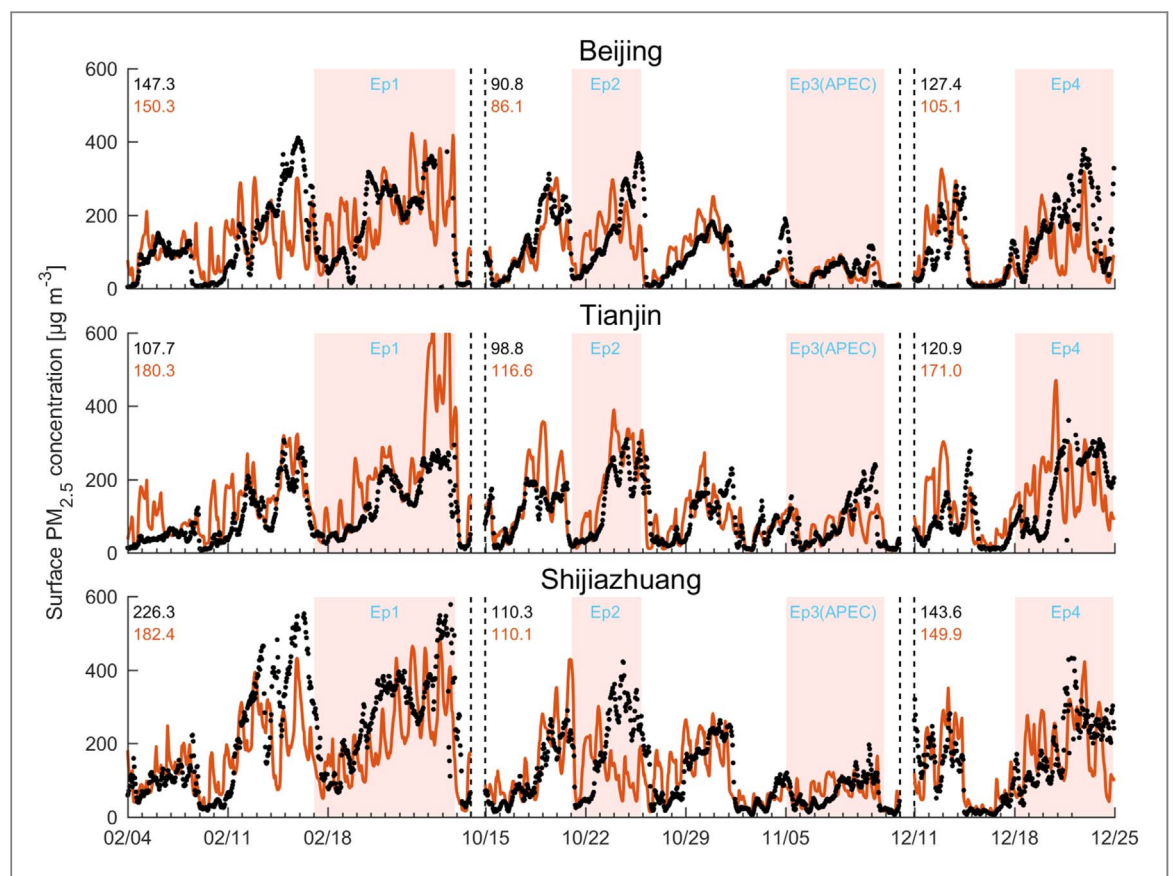


Figure 2. Time series of measured and simulated hourly surface $PM_{2.5}$ concentrations at three megacities (Beijing, Tianjin, and Shijiazhuang) during 4–27 February 2014, 15 October–12 November 2014, and 11–24 December 2015. The shaded areas denote the four episodes analyzed in this study (Ep1–Ep4; Ep3 is the APEC week). Observations (black dots) are compared with model results from the base simulation (red lines). Numbers inset are mean values averaged over the three periods (observations in black and model results in red).

4-27 February 2014, 15 October-12 November 2014, and 11-24 December 2015. We average the hourly measurements at all monitoring sites in a given city to represent the city-level condition. The model captures most of the observed PM_{2.5} temporal variations with correlation coefficients of 0.59-0.64 for the three cities. Model simulated PM_{2,5} concentrations show biases of -17.5%-2.0% at Beijing, 13.3%-57.0% at Tianjin, and -19.4%-4.4% at Shijiazhuang during these periods. The large model overestimates of PM_{2.5} in Tianjin during the last two days of Ep1 is likely due to anomalous southerly wind simulated by the model which is favorable for pollution accumulation. Figure 3 (top panels) shows the spatial distributions of measured and simulated surface PM2.5 concentrations for the four episodes. We can see that in both measurements and model results Ep3 and Ep1 are, respectively, the least and the most polluted cases analyzed in this study. We have also evaluated the model simulated surface temperature, RH, WS, and WD using measurements from the National Climate Data Center (NCDC, https://ncdc.noaa.gov/isd/ data-access), and found no significant biases in the model meteorological fields. Model performance in the base simulation over BTH is summarized in table S2. Figure S2 shows the sea-level pressure and surface wind over North China for the four episodes. We find

that during Ep1 and Ep4 the BTH areas are controlled by high pressure systems leading to stagnant air conditions and pollution accumulation, while during Ep3 (the APEC week) stronger northwestern winds associated a cold surge incursion prevail over BTH.

Previous studies have also shown important influences from both emission reduction and meteorology on PM_{2.5} concentrations in Beijing during the APEC week (Sun et al 2016, Zhang et al 2016, Gao et al 2017, Liang et al 2017). The observed mean PM_{2.5} concentration is 48.9 $\mu g \text{ m}^{-3}$ in Beijing during APEC, and is about 60.3 $\mu \text{g m}^{-3}$ lower than that in previous weeks (109.2 μ g m⁻³ during 15 October–4 November 2014). The simulated corresponding PM_{2.5} concentration reduction in Beijing is 63.7 μ g m⁻³ in this study (104.9 $\mu g \text{ m}^{-3}$ before versus 41.2 $\mu g \text{ m}^{-3}$ during APEC), which is comparable to the observed reduction. Our results also show that if no emission control measures were applied, the mean surface PM_{2.5} concentration in Beijing would be $60.0 \,\mu \mathrm{g \, m^{-3}}$, lower than the simulated mean concentration before APEC (104.9 μ g m⁻³) but higher than the APEC mean in the base simulation (41.2 μ g m⁻³). This supports previous findings that both emission reduction and meteorology are responsible for the PM_{2.5} reduction during APEC (Zhang et al 2016, Gao et al 2017).



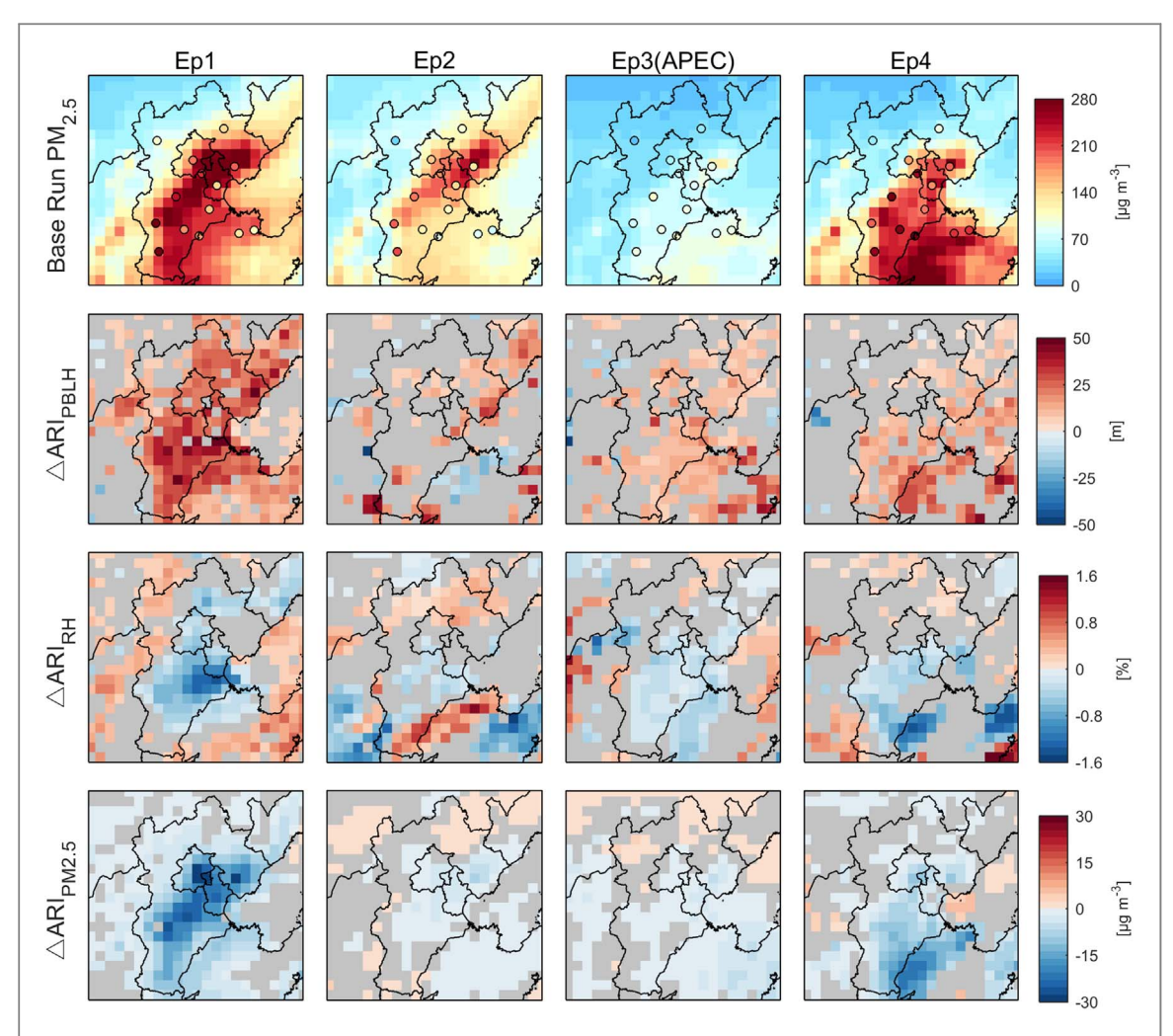


Figure 3. Mean surface PM_{2.5} concentrations for the four episodes (first row). Model results from the base simulation are compared with measurements (circles). The lower three rows show changes in daytime PBLH, daytime 2m RH, and daytime surface PM_{2.5} concentration due to weakened ARI effects when emission control measures are applied. Gray areas denote regions where changes are not statistically significant at 95% confidence level.

3.2. Weakened ARI effects due to emission reductions

We now investigate how ARI can impact the analysis of the effectiveness of emission control measures, e.g. by affecting the attribution of PM_{2.5} changes to emission reduction versus meteorology. Figure 3 shows the spatial distributions of daytime (surface downward shortwave radiation $> 30 \text{ W m}^{-2}$) mean ΔARI_{PBLH} , ΔARI_{RH} , and $\Delta ARI_{PM2.5}$ for the four episodes. We first examine the ARI effects during the APEC week (Ep3) when emission control measures were actually enforced. We find in our sensitivity simulations without emission control that ARI would decrease downward shortwave radiation at the surface by 38 W m⁻² (\sim 10%) on average during APEC over the BTH region, leading to decreases of surface air and skin temperature by -0.4 °C and -1.2 °C, respectively. As a result, it would suppress the development of PBL and increase the APEC daytime mean surface $PM_{2.5}$ concentration by 2.1 μ g m⁻³ over BTH.

Emission reductions lead to weaker impacts of ARI on meteorology and surface PM_{2.5}. As shown in figure 3, during APEC (Ep3) the weaker ARI due to

emission reductions increase the daytime mean PBLH by 0-30 m, and decrease daytime mean 2m RH by 0.7% over the BTH region. These changes in meteorological conditions decrease the regional mean daytime PM_{2.5} concentration by 0.9 μ g m⁻³ (Δ ARI_{PM2.5}). Such effects on surface PM_{2.5} and meteorology are not uniformly distributed as changes in surface winds can affect circulation pattern and also regional transport of moisture and pollutants; the impacts are more prominent in surrounding rural areas where perturbations in local boundary layer processes are relatively small due to lower aerosol loadings. As for the Beijing city, daytime $\triangle ARI_{PM2.5}$ is $-2.2 \mu g \text{ m}^{-3}$, accounting for 8.5% of daytime PM_{2.5} changes due to emission reductions ($\Delta PM_{2.5}$, $-25.9 \mu g m^{-3}$). Considering both daytime and nighttime values, $\Delta ARI_{PM2.5}$ and $\Delta ARI_{PM2.5}/\Delta PM_{2.5}$ for Ep3 are $-1.8 \ \mu g \ m^{-3}$ and 6.7%, respectively (table 2). These are consistent with a recent WRF-Chem study that estimated a decrease of $1.9 \,\mu\mathrm{g}\,\mathrm{m}^{-3}$ in daytime mean surface PM_{2.5} concentration in Beijing due to the weakened ARI effect during APEC (Gao et al 2017).



Table 2. PM_{2.5} concentrations and ARI effects in urban Beijing during the four episodes.

Episode	Ep1	Ep2	Ep3 (APEC)	Ep4
Period	17–26 February 2014	21–25 October 2014	05–11 November 2014	18–24 December 2015
$PM_{2.5} (\mu g m^{-3})^a$	282.1	118.6	77.0	158.4
$\Delta ARI_{PM2.5} (\mu g m^{-3})^b$	-22.2	-2.5	-1.8	-6.6
$\Delta PM_{2.5}^* (\mu g m^{-3})$	-79.4	-30.5	-24.6	-60.8
$\Delta PM_{2.5} (\mu g m^{-3})$	-101.6	-33.0	-26.4	-67.3
Δ ARI $_{PM2.5}/\Delta$ PM $_{2.5}$ (%) c	21.9%	7.5%	6.7%	9.7%

 $^{^{\}rm a}\,$ Model results from Run A with ARI turned on and emission reduction turned off.

Larger impacts due to the weakened ARI effects can be seen in figure 3 for other episodes. In the most polluted episode (Ep1), emission reductions would increase the daytime mean PBLH by up to 48 m over BTH. The resulting decreases in the daytime mean PM_{2.5} concentration over BTH average 10.2 μ g m⁻³, much higher than other episodes. The Δ ARI_{PM2.5}/ Δ PM_{2.5} ratio for Beijing during Ep1 reaches 21.9% (table 2), indicating a significant percentage underestimation of the PM_{2.5} concentration reduction due to emission control measures in a model simulation without ARI considered.

Analyses of the four episodes together indicate that the impacts of ARI intensify dramatically as increasing PM_{2.5} concentrations in the BTH region. Figure S1 shows the relationships of daytime surface PM2.5 concentrations (model results from Run A) versus ARI induced meteorological perturbations for the ensemble of four episodes and the BTH grid cells. Reduced surface downward shortwave radiation due to ARI shows a linear relationship with surface PM_{2.5} concentrations (figure S1(a)). This linear relationship is consistent with observations of surface PM25 concentration and solar radiation in Beijing as shown by Liu et al (2018). Decreases in PBLH due to ARI follow a quadratic relationship with surface PM_{2.5} concentrations (figure S1(b)), reflecting a positive feedback between the two. It leads to a robust quadratic relationship ($R^2 = 0.94$) between surface PM_{2.5} concentrations and ARI induced PM2.5 concentration changes over BTH during the four episodes as shown in figure 4(a). Additional positive feedback can be caused by changes in other meteorological variables, such as RH. Decreases in downward solar radiation tend to decrease surface temperature and increase RH (figure S1(c)), leading to conditions favorable for secondary aerosol formation (Liu et al 2018).

The quadratic relationship of ARI effects to PM_{2.5} concentrations can have an important implication for assessing the effectiveness of emission control measures. Figure 4(b) shows how PM_{2.5} concentrations over the BTH region would decrease if emission reductions are applied with or without ARI considered. We can see that if there were no ARI, surface PM_{2.5} would decrease approximately linearly (a

quadratic fitting term would be very small and statistically insignificant at 95% confidence level) relative to their concentrations over BTH. However, with ARI, the impacts of emission reductions enhance in a distinct quadratic way (a quadratic fitting could increase R^2 by 0.005 and the quadratic term is statistically significant at 95% confidence level) as increasing surface PM_{2.5} concentrations. Under heavy polluted conditions, changes in ARI associated with emission reductions would lead to a greater improvement of air quality than we would expect in the absence of ARI. This is also shown in figure 4(c) that the $\Delta ARI_{PM2.5}/\Delta PM_{2.5}$ metric, defined for quantifying the impact of ARI on the effectiveness of emission control measures, increases as increasing surface PM_{2.5} concentrations. As summarized in table 2, emission reductions would decrease episodic mean PM2.5 concentrations in Beijing by 26.4–101.6 μ g m⁻³ with ARI considered, and by 24.6–79.4 μ g m⁻³ without ARI considered, leading to 6.7%-21.9% differences for the estimates of their effectiveness.

We further discuss two uncertainties that might affect the model simulated PM_{2.5} responses to emission reductions. First, the influences of ACI are not considered by fixing CDNC to 10 cm⁻³ in the model that typically represent pristine conditions away from continents (Zeng et al 2014). Over more polluted regions such as BTH, aerosols can enhance CDNC and further affect cloud and precipitation conditions. Satellite retrievals showed that the annual mean CDNC could reach 200 cm⁻³ in this region (Zeng et al 2014). Second, the dependence of PM_{2.5} responses to model horizontal resolution is not clear. Here we conduct two additional sensitivity simulations for both Ep1 (the most polluted episode analyzed in this study) and Ep2 (a moderate polluted episode): one by altering prescribed CDNC from 10 to 200 cm⁻³, and the other by using the WRF-Chem nested capability and increasing the resolution from 36 km to 12 km over the BTH region (figure 1). Figures S3 and S4 compare the ARI effects as analyzed above (in figures 3 and 4) with those simulated in the two additional sensitivity simulations. We can see that changing the CDNC value and the model horizontal resolution lead to

^b Δ ARI_{PM2.5} is calculated as model results of [(Run B - Run D) - (Run A - Run C)], Δ PM_{2.5}* is from (Run D - Run C), and Δ PM_{2.5} is from (Run B - Run A).

^c Values show the impacts of ARI on the effectiveness of emission control measures.

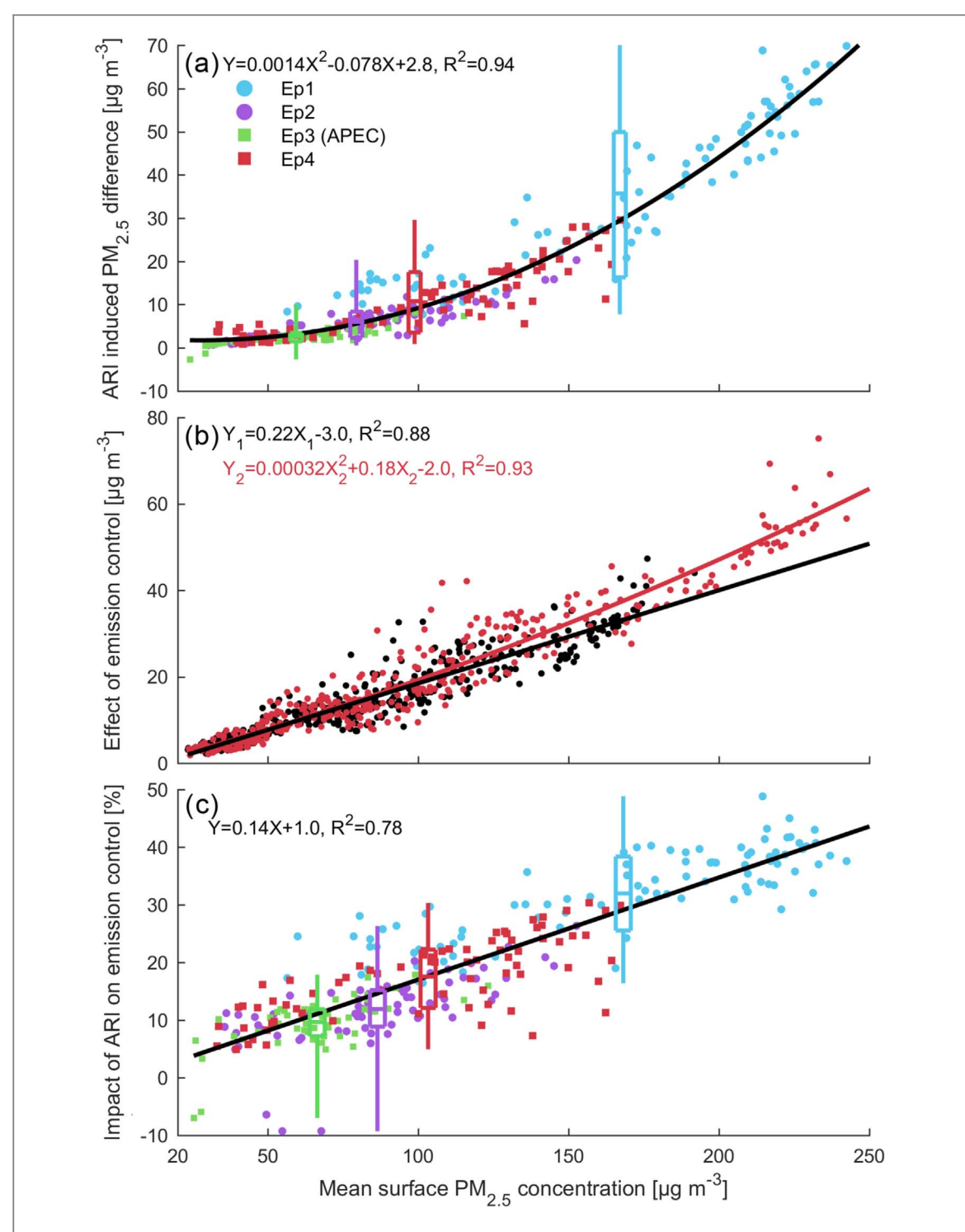


Figure 4. The relationships of daytime surface $PM_{2.5}$ concentrations (model results from Run A) versus $PM_{2.5}$ concentration changes due to ARI effects and emission reductions for the ensemble of four episodes. Each point represents the episodic mean in a BTH grid cell. Panel (a) shows the relationship versus ARI induced $PM_{2.5}$ concentration changes (Run A minus Run C). Panel (b) shows the relationship versus $PM_{2.5}$ reductions due to emission reductions (Run A minus Run B in red with ARI, and Run C minus Run D in black without ARI). $PM_{2.5}$ concentrations in this panel are from Run A (red) and Run C (black). Panel (c) shows the relationship versus the impact of ARI on the effectiveness of emission control ($\Delta ARI_{PM2.5}/\Delta PM_{2.5}$ in the text). The box-and-whisker plots denote minimum, 25th, 50th, 75th percentiles, and maximum values for each episode. Linear or quadratic fitting lines are shown inset. Note that a quadratic fitting for the black dots in panel b would be statistically insignificant.

small differences and do not affect our results. Model results show larger effects from increasing horizontal resolution than that of CDNC (e.g. reversed responses of PBLH in the southern edge of BTH during Ep2 in figure S3 and decreased R^2 in figure S4(c)). ACI can also affect surface PM_{2.5} levels. On one hand, via

altering cloud properties including CDNC, albedo, and lifetime, ACI perturbs downward solar radiation and further changes boundary layer process as ARI does. On the other hand, it enhances secondary aerosol formation through cloud chemistry (Zhao *et al* 2017). The inclusion of ACI would lead to increments



to $PM_{2.5}$ concentrations in all scenarios and might further decrease surface $PM_{2.5}$ concentrations when emission controls are applied. Future work is needed to better represent the model ACI effects and assess their changes associated with emission reductions.

4. Conclusion

In summary, we have investigated the impact of ARI on surface PM_{2.5} concentration changes assuming temporary emission control measures are applied over the BTH region. Four episodes in 2014 and 2015 are analyzed covering a wide range of PM_{2.5} pollution conditions in BTH. We show that if there were no ARI, an emission reduction would decrease surface PM_{2.5} approximately in a linear relationship with its concentration. However, with ARI a quadratic relationship exists between surface PM_{2.5} concentrations and their decreases due to the emission reduction. This implies that emission control measures can be much more effective under heavy pollution conditions due to the ARI effects. For the four analyzed episodes, mean surface PM_{2.5} decreases in Beijing due to emission reductions can be 6.7%-21.9% larger than those estimated without ARI. Our study emphasizes the need to account for aerosol-meteorology interactions when designing short-term emission control measures and assessing their effectiveness.

Acknowledgments

This work was funded by the National Key Research and Development Program of China (2017YFC0210102) and China's National Basic Research Program (2014CB441303). YG and BZ are supported by the NSF grant AGS-1701526. YG also acknowledges the support of the Natural Science Foundation of Jiangsu Province, China (No. BK20171230).

ORCID iDs

Mi Zhou https://orcid.org/0000-0001-8600-1503 Lin Zhang https://orcid.org/0000-0003-2383-8431 Dan Chen https://orcid.org/0000-0002-6317-0707 Yu Gu https://orcid.org/0000-0002-3412-0794 Meng Gao https://orcid.org/0000-0002-8657-3541 Xiao Lu https://orcid.org/0000-0002-5989-0912

References

- Andreae M O *et al* 2008 Aerosol–cloud–precipitation interactions: I.

 The nature and sources of cloud-active aerosols *Earth Sci. Rev.* 89 13–41
- Boucher O et al 2013 Clouds and aerosols Climate Change 2013: The Physical Science Basis. Contribution of Working Group I to the Fifth Assessment Report of the Intergovernmental Panel on Climate Change ed T F Stocker et al (Cambridge: Cambridge University Press) pp 571–658

- Chapman E G et al 2009 Coupling aerosol–cloud-radiative processes in the WRF-Chem model: investigating the radiative impact of elevated point sources Atmos. Chem. Phys. 9 945–64
- Chen D et al 2016 Simulations of sulfate-nitrate-ammonium (SNA) aerosols during the extreme haze events over northern China in October 2014 Atmos. Chem. Phys. 16 10707–24
- Chen F *et al* 2001 Coupling an advanced land surface hydrology model with the penn state NCAR MM5 modeling system: I. Model implementation and sensitivity *Mon. Weather Rev.* 129 569–85
- Fast J et al 2006 Evolution of ozone, particulates, and aerosol direct radiative forcing in the vicinity of Houston using a fully coupled meteorology-chemistry-aerosol model J. Geophys. Res.-Atmos. 111 D21305
- Gao M et al 2017 Distinguishing the roles of meteorology, emission control measures, regional transport, and co-benefits of reduced aerosol feedbacks in 'APEC Blue' Atmos. Environ. 167 476–86
- Gao Y et al 2015 Modeling the feedback between aerosol and meteorological variables in the atmospheric boundary layer during a severe fog-haze event over the North China Plain Atmos. Chem. Phys. 15 1093–130
- Grell G A et al 2005 Fully coupled 'online' chemistry within the WRF model Atmos. Environ. 39 6957–75
- Guenther A et al 2006 Estimates of global terrestrial isoprene emissions using MEGAN (model of emissions of gases and aerosols from nature) Atmos. Chem. Phys. 6 3181–210
- Guo J P et al 2016 Impact of various emission control schemes on air quality using WRF-Chem during APEC China 2014 Atmos. Environ. 140 311–9
- Gustafson W I et al 2007 Impact on modeled cloud characteristics due to simplified treatment of uniform cloud condensation nuclei during NEAQS 2004 Geophys. Res. Lett. 34 255–68
- Hansen J et al 1997 Radiative forcing and climate response J. Geophys. Res.-Atmos. 102 6831–64
- Hong S-Y et al 2006 A new vertical diffusion package with an explicit treatment of entrainment processes Mon. Weather Rev. 134 2318
- Jones S L et al 2012 Update on modifications to WRF-CHEM GOCART for fine-scale dust forecasting at AFWA AGU Fall Meeting Abstracts
- Li M *et al* 2017b MIX: a mosaic Asian anthropogenic emission inventory under the international collaboration framework of the MICS-Asia and HTAP *Atmos. Chem. Phys.* 17 34813–69
- Li Z Q et al 2017a Aerosol and boundary-layer interactions and impact on air quality Natl. Sci. Rev. 6 810–33
- Liang P F et al 2017 The role of meteorological conditions and pollution control strategies in reducing air pollution in Beijing during APEC 2014 and Victory Parade 2015 Atmos. Chem. Phys. 17 1–62
- Liu Q et al 2018 New positive feedback mechanism between boundary layer meteorology and secondary aerosol formation during severe haze events Sci. Rep. 8 6095
- Lelieveld J et al 2015 The contribution of outdoor air pollution sources to premature mortality on a global scale Nature 525 367–71
- Morrison H et al 2005 Mesoscale modeling of springtime arctic mixed-phase stratiform clouds using a new two-moment bulk microphysics scheme J. Atmos. Sci. 62 3683–704
- Qiu Y L et al 2017 Simulated impacts of direct radiative effects of scattering and absorbing aerosols on surface layer aerosol concentrations in China during a heavily polluted event in February 2014 J. Geophys. Res.-Atmos. 122 5955–75
- Ramanathan V $\it et\,al\,2001$ Aerosols, climate, and the hydrological cycle $\it Science\,294\,2119-24$
- Sun Y L et al 2016 'APEC blue': secondary aerosol reductions from emission controls in Beijing Sci. Rep. 6 20668
- Wang S X *et al* 2014 Impact of aerosol—meteorology interactions on fine particle pollution during China's severe haze episode in January 2013 *Environ. Res. Lett.* **9** 094002



- Yang X et al 2016 Intensification of aerosol pollution associated with its feedback with surface solar radiation and winds in Beijing J. Geophys. Res.-Atmos. 121 4093–9
- Yang Y R et al 2015 Characteristics and formation mechanism of continuous hazes in China: a case study during the autumn of 2014 in the North China Plain Atmos. Chem. Phys. 15 10987–1029
- Zaveri R A et al 1999 A new lumped structure photochemical mechanism for large-scale applications J. Geophys. Res.-Atmos. 104 30387–415
- Zaveri R A et al 2008 Model for simulating aerosol interactions and chemistry (MOSAIC) J. Geophys. Res.-Atmos. 113 D13204
- Zeng S et al 2014 Study of global cloud droplet number concentration with A-Train satellites Atmos. Chem. Phys. 14 7125–34
- Zhang L et al 2015a Source attribution of particulate matter pollution over North China with the adjoint method *Environ*. Res. Lett. 10 084011

- Zhang B *et al* 2015b Simulating aerosol–radiation-cloud feedbacks on meteorology and air quality over eastern China under severe haze conditions in winter *Atmos. Chem. Phys.* **15** 2387–404
- Zhang L et al 2016 Sources and processes affecting fine particulate matter pollution over North China: an adjoint analysis of the Beijing APEC period Environ. Sci. Technol. 50 8731–40
- Zhang X et al 2018 Enhancement of PM_{2.5} concentrations by aerosol–meteorology interactions over China J. Geophys. Res.-Atmos. 123 1179–94
- Zhao B et al 2017 Enhanced PM_{2.5} pollution in China due to aerosol–cloud interactions Sci. Rep. 7 4453
- Zhong J T et al 2018 Feedback effects of boundary-layer meteorological factors on explosive growth of PM $_{2.5}$ during winter heavy pollution episodes in Beijing from 2013 to 2016 Atmos. Chem. Phys. 18 247–58